

# Fabrication trueness and internal fit of different lithium disilicate ceramics according to post-milling firing and material type

Münir Demirel<sup>a</sup>, Mustafa Borga Donmez<sup>b,c,\*</sup>

<sup>a</sup> Department of Prosthodontics, Faculty of Dentistry, Biruni University, Istanbul, Turkey

<sup>b</sup> Department of Prosthodontics, Faculty of Dentistry, Istinye University, Istanbul, Turkey

<sup>c</sup> Department of Reconstructive Dentistry and Gerodontology, School of Dental Medicine, University of Bern, Bern, Switzerland

## ARTICLE INFO

### Keywords:

Crystallization  
Fabrication trueness  
Lithium disilicate  
Internal fit  
Matrix firing

## ABSTRACT

**Objectives:** To evaluate whether post-milling firing and material type affect the fabrication trueness and internal fit of lithium disilicate crowns.

**Methods:** A prefabricated cobalt chromium abutment was digitized to design a mandibular right first molar crown. This design file was used to fabricate crowns from different lithium disilicate ceramics (nano-lithium disilicate (AM), fully crystallized lithium disilicate (IN), advanced lithium disilicate (TS), and lithium disilicate (EX)) ( $n = 10$ ). Crowns, the abutment, and the crowns when seated on the abutment were digitized by using an intraoral scanner. Fabrication trueness was assessed by using the root mean square method, while the internal fit was evaluated according to the triple scan method. These processes were repeated after the post-milling firing of AM, TS, and EX. Paired samples *t*-tests were used to analyze the effect of post-milling firing within AM, TS, and EX, while all materials were compared with 1-way analysis of variance and Tukey HSD tests ( $\alpha = 0.05$ ).

**Results:** Post-milling firing reduced the surface deviations and internal gap of AM and EX ( $P \leq 0.014$ ). AM mostly had higher deviations and internal gaps than other materials ( $P \leq 0.030$ ).

**Conclusions:** Post-milling firing increased the trueness and internal fit of tested nano-lithium disilicate and lithium disilicate ceramics. Nano-lithium disilicate mostly had lower trueness and higher internal gap; however, the maximum meaningful differences among tested materials were small. Therefore, the adjustment duration and clinical fit of tested crowns may be similar.

**Clinical Significance:** Tested lithium disilicate ceramics may be suitable alternatives to one another in terms of fabrication trueness and internal fit, considering the small differences in measured deviations and internal gaps.

## 1. Introduction

Along with the implementation of computer-aided design and computer-aided manufacturing (CAD-CAM) systems into dentistry, lithium disilicate ceramics have become one of the most commonly preferred materials for esthetic restorations ever since the introduction of IPS e.max CAD (EX, Ivoclar AG, Schaan, Liechtenstein) in early 21st century [1,2], given their pleasing esthetic and mechanical properties [3,4]. However, the number of available materials in the dental market is constantly increasing, and after the patent expiration of EX in 2019 [5], new lithium disilicate ceramics with different properties and crystalline structures have started to be introduced [6,7]. Among these new materials, nano-lithium disilicate has a unique feature of translucency

adjustment based on crystallization firing temperature [8,9]. Another new material is advanced lithium disilicate, which has a secondary crystal called virgilitite in its chemical composition along with lithium disilicate [10]. This new material also has the advantage of a shorter post-milling process when the proprietary furnace of the manufacturer (CEREC SpeedFire; Dentsply Sirona, Bensheim, Germany) is used for the mandatory matrix firing that may also involve glazing [6]. CAD-CAM blocks that do not need any crystallization firing have also recently been marketed as fully crystallized lithium disilicate (Initial LiSi Block; GC Corp, Tokyo, Japan) and can be delivered after milling and polishing [7,11].

CAD-CAM systems and lithium disilicate ceramics have facilitated prosthetic rehabilitation to be completed in a single appointment [12].

\* Corresponding author: Department of Reconstructive Dentistry and Gerodontology, School of Dental Medicine, University of Bern, Freiburgstrasse 7 3007 Bern, Switzerland

E-mail address: [mustafa-borga.doenmez@unibe.ch](mailto:mustafa-borga.doenmez@unibe.ch) (M.B. Donmez).

<https://doi.org/10.1016/j.jdent.2024.104987>

Received 17 January 2024; Received in revised form 29 March 2024; Accepted 2 April 2024

Available online 3 April 2024

0300-5712/© 2024 The Author(s). Published by Elsevier Ltd. This is an open access article under the CC BY license (<http://creativecommons.org/licenses/by/4.0/>).

However, this trend increased the importance of fabricating prostheses that have the utmost congruence with the CAD file, which not only minimizes the number of adjustments required but also increases the internal fit of the prostheses [13]. As mentioned above, some of the available lithium disilicate ceramics require a post-milling firing before further processes and the manufacturer of EX has disclosed a 0.2 % densification during crystallization [12,14–16]; however, to the authors' knowledge, whether nano-lithium disilicate or advanced lithium disilicate undergoes a similar linear shrinkage after post-milling firing has not been disclosed.

The studies on newly introduced lithium disilicate ceramics have mainly focused on their optical or mechanical properties [4,6–10, 17–21]. The authors are aware of only 4 studies that investigated the fabrication trueness of those newly introduced lithium disilicate ceramics [11,22–24]. However, none of those studies investigated the internal fit of lithium disilicate ceramics and involved the effect of post-milling firing (crystallization or matrix firing) on the fabrication trueness of newly introduced lithium disilicate ceramics. Considering that currently available lithium disilicate ceramics differ in chemical composition, crystalline structure, and crystalline size, a study based on the fabrication trueness and internal fit of different lithium disilicate ceramics may elaborate the knowledge of clinicians and dental technicians on these materials and facilitate their implementation into clinical practice. In addition, dental laboratories and clinicians may benefit from the fit evaluation of prostheses on master casts immediately after fabrication to facilitate the preparations for try-in appointments by using readily available equipment such as laboratory scanners or intraoral scanners (IOSs) to generate the test scans. Therefore, the present study aimed to evaluate the effect of post-milling firing and material type on the fabrication trueness and internal fit of newly introduced lithium disilicate ceramics by comparing them with well-established EX. The null hypotheses were that i) post-milling firing would not affect the fabrication trueness of lithium disilicate ceramics that require crystallization or matrix firing, ii) post-milling firing would not affect the internal fit of lithium disilicate ceramics that require crystallization or matrix firing, iii) material type would not affect the fabrication trueness of lithium disilicate ceramics, and iv) material type would not affect the internal fit of lithium disilicate ceramics.

## 2. Material and methods

The number of specimens was decided based on a priori power analysis (G\*Power v3.1; Heinrich Heine University of Düsseldorf, Düsseldorf, Germany), which yielded a minimum of 4 specimens sufficient (for 95 % CI (1- $\alpha$ ), 95 % power (1- $\beta$ ), and effect size of  $f = 1.67$ ) [16]. However, 10 crowns per material were fabricated to increase the statistical power. One nano-lithium disilicate (Amber Mill; HASSBio, Kangneung, Korea (AM)), one fully crystallized lithium disilicate (Initial LiSi Block; GC Corp, Tokyo, Japan (IN)), one advanced lithium disilicate (CEREC Tessera; Dentsply Sirona, Bensheim, Germany (TS)), and one lithium disilicate (IPS e.max CAD; Ivoclar AG, Schaan, Liechtenstein (EX)), which are elaborated in Table 1, were tested in the present study. Other than AM, all specimens were fabricated by using A2-shaded highly translucent blocks, while AM specimens were fabricated by using A2-shaded blocks, which were crystallized to achieve high translucency.

A prefabricated 7.5 mm-long cobalt chromium abutment with 1 mm-thick shoulder finish line and 12° convergence on a base with 3 hemispheres placed at the corners was digitized by using a laboratory scanner (inEos X5; Dentsply Sirona, Bensheim, Germany) to generate its standard tessellation language (STL) file. This STL file was then imported into a dental design software program (CEREC inLab CAD SW 20.0.3; Dentsply Sirona, Bensheim, Germany) and a mandibular right first molar crown with 80  $\mu$ m cement space [25] was designed in STL format (Fig. 1). Other parameters were 25  $\mu$ m of proximal, occlusal, and dynamic contact strength, 50  $\mu$ m of margin thickness, 1 mm of minimum axial thickness, and 1.5 mm of minimum occlusal thickness. This master

**Table 1**

List of lithium disilicate ceramics tested in this study.

Material	Chemical Composition (wt %)	Crystal Size	Manufacturer
Amber Mill (Nano-lithium disilicate, AM)	SiO <sub>2</sub> : <78 % Li <sub>2</sub> O: <12 % Coloring oxides: <12 %	0.2 $\mu$ m	HASSBio, Kangneung, Korea
Initial LiSi Block (Fully crystallized lithium disilicate, IN)	SiO <sub>2</sub> : 81 % P <sub>2</sub> O <sub>5</sub> : 8.1 % K <sub>2</sub> O: 5.9 % Al <sub>2</sub> O <sub>3</sub> : 3.8 % TiO <sub>2</sub> : 0.5 % CeO <sub>2</sub> : 0.6 %	1–1.5 $\mu$ m	GC Corp, Tokyo, Japan
CEREC Tessera (Advanced lithium disilicate, TS)	Li <sub>2</sub> Si <sub>2</sub> O <sub>5</sub> : 90 % Li <sub>3</sub> PO <sub>4</sub> : 5 % Li <sub>0.5</sub> Al <sub>0.5</sub> Si <sub>2.5</sub> O <sub>6</sub> (virgillite): 5 %	0.5 $\mu$ m lithium disilicate and 0.2–0.3 $\mu$ m virgillite	Dentsply Sirona, Bensheim, Germany
IPS e.max CAD (Lithium disilicate, EX)	SiO <sub>2</sub> : 57–80 % Li <sub>2</sub> O: 11–19 % K <sub>2</sub> O: 0–13 % P <sub>2</sub> O <sub>5</sub> : 0–11 % ZrO <sub>2</sub> : 0–8 % ZnO: 0–8 % Coloring oxides: 0–8 %	1–1.5 $\mu$ m	Ivoclar AG, Schaan, Liechtenstein

STL (M-STL) was then imported into a nesting software program (CEREC inLab CAM SW 20.0.1; Dentsply Sirona, Bensheim, Germany) to mill lithium disilicate crowns with a 4-axis milling unit (CEREC Primemill; Dentsply Sirona, Bensheim, Germany) in normal machining mode with high details. A new set of burs (Diamond 1.2 and Diamond 1.4; Dentsply Sirona, Bensheim, Germany) was used for each group. After fabrication, a single operator (M.D.) removed the supports on the external surfaces of the crowns with a cut-off wheel, which were then gently smoothed with a small round bur by using optical magnification loupes (EyeMag Pro; Carl Zeiss, Oberkochen, Germany) under  $\times 3.5$  magnification. Crowns were then ultrasonically cleaned for 10 min in distilled water.

All crowns were randomly (Excel; Microsoft Corp, Seattle, WA, USA) digitized by using an IOS (CEREC Primescan SW 5.2; Dentsply Sirona, Bensheim, Germany). IOS was calibrated before the scans and recalibrated after every 5 scans until all crowns were digitized to generate test scan STLs (T-STLs). In addition, fatigue-related deviations were minimized as the operator (M.D.) took 5-minute breaks after every 5 scans [26], and all scans were performed in the same temperature- (20 °C) and humidity-controlled (45 %) room in which the cobalt-chromium abutment was digitized. The room was lit by sunlight. The abutment and its base were also digitized by using the same IOS to generate its STL file (A-STL). Finally, each crown was seated on the abutment and this complex was digitized with the same IOS to generate crown-on-abutment STLs (C-STLs). Precrystallized AM, TS, and EX crowns were then crystallized in a porcelain furnace (Programat P300; Ivoclar AG, Schaan, Liechtenstein) in line with their respective manufacturers' recommendations (Table 2). Fired crowns were also ultrasonically cleaned for 10 min in distilled water, and were digitized as mentioned above to generate their T-STL and C-STL files. Regardless of the presence of the post-milling firing, no additional glazing or polishing was performed on any of the crowns [26–29] as any human intervention would have affected the measured deviations from the original CAD data.

T-STLs and M-STL were imported into a 3-dimensional analysis software program (Medit Link v3.0.6; Medit, Seoul, Korea) to evaluate the fabrication trueness of lithium disilicate crowns [26,27,30]. To superimpose T-STL over the M-STL, 3 points (one point on the mesial triangular fossa, one point on the distal triangular fossa, and one point on the central sulcus) were simultaneously selected on both files. To quantitatively evaluate deviations, color maps with maximum and minimum nominal values set at +100  $\mu$ m and –100  $\mu$ m and the

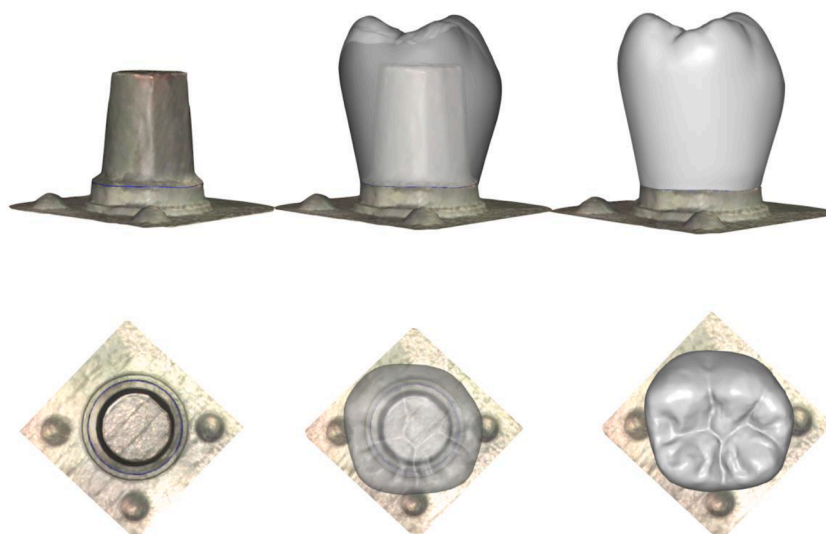


Fig. 1. Digitized abutment and crown design from proximal and occlusal aspects.

Table 2

Post-milling firing parameters used in this study. AM, Nano-lithium disilicate; B, Stand-by temperature; EX, Lithium disilicate; L, Long-term cooling; S, Closing time; t1/t2, Heating rate; T1/T2, Holding temperature; TS, Advanced lithium disilicate; Vac. 1, Vacuum 1; Vac. 2, Vacuum 2.

	B [°C]	S [min]	t1/t2 [°C/ min]	T1/T2 [°C]	H1/H2 [min]	Vac. 1 [°C]	Vac. 2 [°C]	L [°C]
AM	400 °C	3 min	60 °C/ min	815 °C	15 min	550 °C 815 °C	0	690 °C
TS	403 °C	2 min	55 °C/ min	760 °C	2 min	550 °C -830 °C	0	0
EX	403 °C	6 min	90/34 °C/min	830/ 850 °C	10 s/7 min	550 °C -830 °C -850 °C		710 °C

tolerance range set at +10 μm and -10 μm were generated [31]. Root mean square (RMS) values were automatically calculated by the software program for the qualitative evaluation of overall deviations [32]. STL files were imported again and external, intaglio, and marginal surfaces were virtually separated to further analyze deviations [26] (Figs. 2 and 3). T-STLs, C-STLs, and A-STL were imported into the same analysis software program to evaluate internal fit by using the triple scan method [28,29]. C-STL was initially superimposed over the A-STL by selecting 1 point on each of the spheres at the base. Then, T-STL was superimposed over this merged STL by selecting 3 points on the occlusal surface of the crowns (one point on the mesial triangular fossa, one point on the distal triangular fossa, and one point on the central sulcus), similar to fabrication trueness analyses. These consecutive superimpositions merged T-STL, C-STL, and A-STL on the same coordinate system and C-STL was deleted after superimpositions were completed. The average gaps between the intaglio surface of the crowns and the abutment surface were automatically calculated (Figs. 4 and 5). All deviation and average gap analyses were performed by a single operator (M.D.).

The normality of data was assessed by using Kolmogorov-Smirnov tests, while the homogeneity of variances was assessed with Leven's test. These tests showed that data had normal distribution and the variances were distributed homogeneously. Paired samples *t*-tests were used to evaluate the effect of post-milling firing on the fabrication trueness and internal fit of AM, TS, and EX. One-way analysis of variance (ANOVA) and Tukey HSD tests were used to compare the RMS values at each surface and average gap values among tested materials. All

statistical analyses were performed by using a statistical analysis software program (SPSS v23; IBM Corp, Armonk, NY, USA) with the significance level set at  $\alpha = 0.05$ .

### 3. Results

Table 3 shows the descriptive statistics of RMS values of AM, TS, and EX before and after post-milling firing. Regardless of the surface, post-milling firing did not affect the RMS values of TS ( $P \geq .217$ ), whereas AM and EX had higher deviations before post-milling firing within each surface ( $P \leq 0.014$ ). AM and EX had lower average gap values after post-milling firing ( $P < .001$ ). However, post-milling firing did not affect the average gap values of TS ( $P = .845$ ) (Table 4).

Table 5 lists the descriptive statistics of RMS values for each material-surface pair. One-way ANOVAs showed significant differences among tested materials within each surface ( $P \leq 0.011$ ). When the overall RMS was considered, AM had the highest deviations ( $P \leq 0.030$ ). When the external and marginal surface RMS values were considered, AM had higher deviations than EX and IN ( $P \leq 0.024$ ). When the intaglio surface RMS was considered, EX had lower deviations than TS and AM ( $P \leq 0.038$ ). The differences among materials when average gap values were considered were significant ( $P < .001$ ) as AM had higher average gap values than TS and IN ( $P \leq 0.001$ ) (Table 6).

### 4. Discussion

Post-milling firing increased the fabrication trueness and internal fit of AM and EX, which led to the rejection of the first and the second null hypotheses. Color maps of AM, TS, and EX represent the fact that these materials were milled larger than the CAD file as red, orange, and yellow, which represent overcontoured areas of different intensities, were dominant on most of the external and occlusal surfaces of the crowns. Considering that red was also visible on the axial walls of the intaglio surfaces and the same color scheme was evident on the marginal surfaces, a possible misfit might be encountered at this stage, particularly for AM and EX as they also had higher gaps before post-milling firing, which supports this hypothesis. Intraoral adjustment of EX crowns before crystallization has been reported [33]; however, based on the results of the present study, this process might lead to open contacts after crystallization and should be avoided, particularly in the case of multiple adjacent restorations. Before and after post-milling firing color maps of TS were almost identical, which is in line with the measured deviations as post-milling firing did not affect the surface trueness of TS.

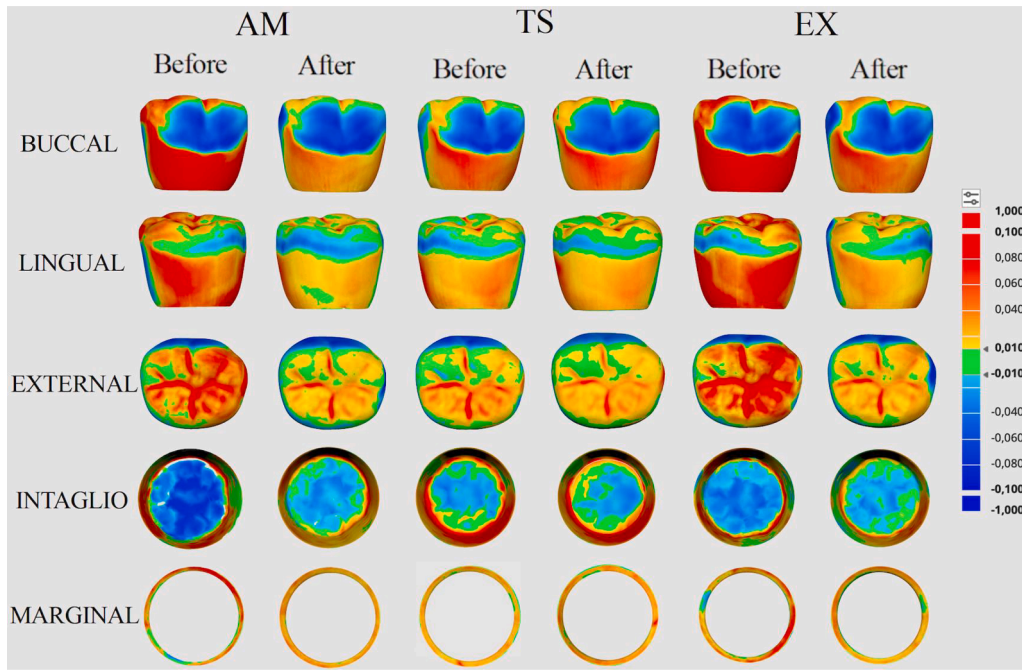


Fig. 2. Representative color maps generated after superimposition for materials that require post-milling firing.

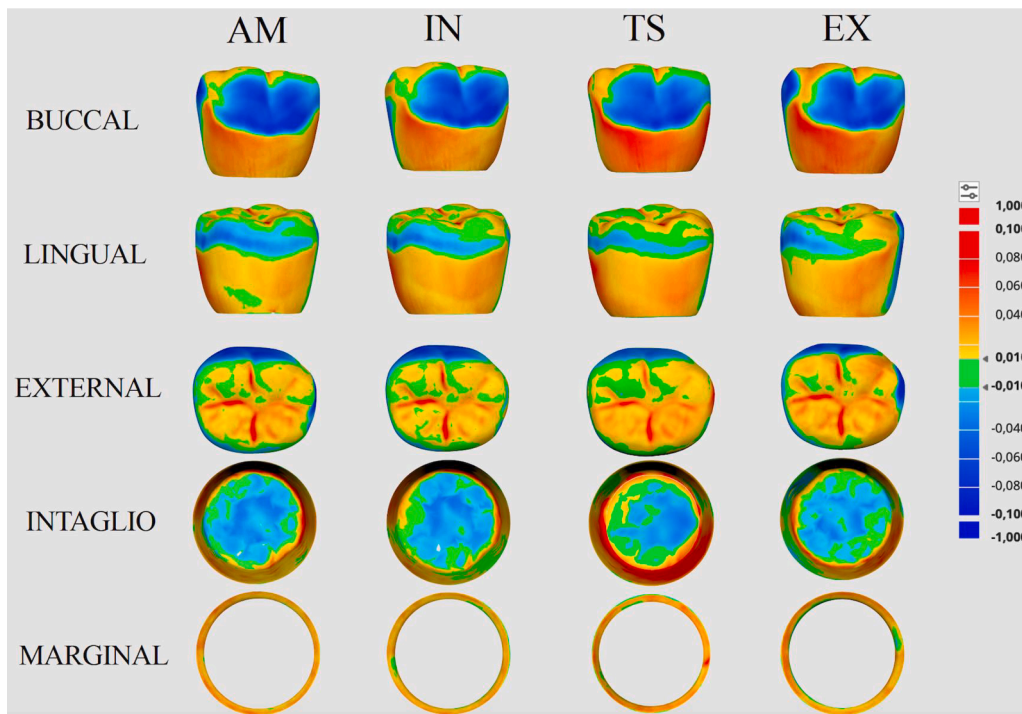


Fig. 3. Representative color maps generated after superimposition from each material-surface pair.

However, the color distribution on the external surface of TS changed with post-milling firing, and when the occlusal surface was evaluated, the intensity of red at the buccal inclination of the lingual cusps was not that evident after post-milling firing. The chemical composition of AM, TS, and EX may be related to the different behavior of these materials to post-milling firing as TS comprises virgilitic crystals, which are not present in AM and EX. Post-milling firing parameters may be another factor that contributed to this difference as TS has a lower final temperature and the firing process does not involve vacuum.

The authors think that the present study was the first on the effect of

post-milling firing on fabrication trueness and internal fit of AM and TS; therefore, comparison with previous studies was not possible. Yamamoto et al. [22] evaluated the effect of crystallization fabrication trueness of EX by using an analysis software program and concluded that crystallization reduced the trueness of the crowns. This difference between the present and Yamamoto et al. [22] studies may be related to the fact that a different milling unit was used to fabricate the crowns with a different design to those of the present study, an optical precision measuring machine (ATOS Capsule; GOM, Braunschweig, Germany) was used to generate test scan data, and another software program

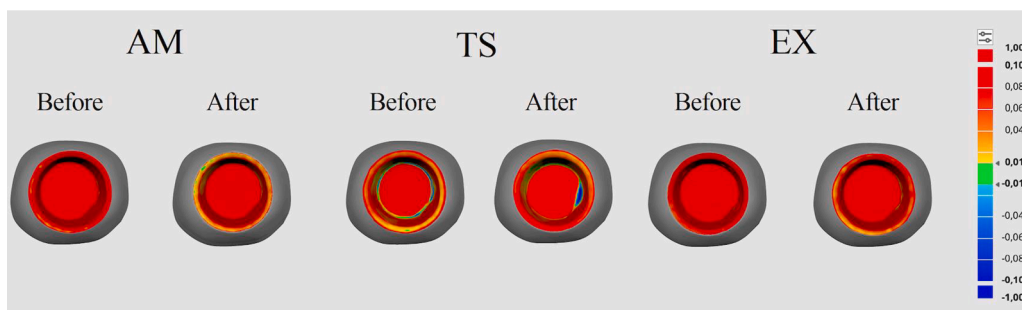


Fig. 4. Representative color maps generated after superimpositions according to triple scan method for materials that require post-milling firing.

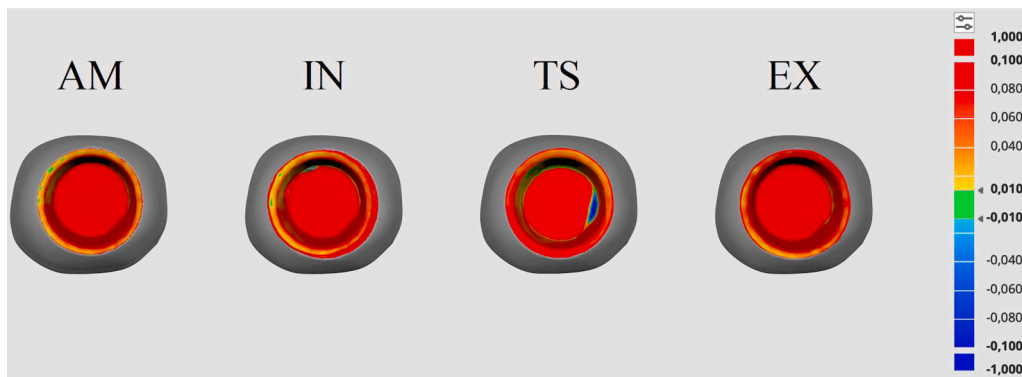


Fig. 5. Representative color maps generated after superimpositions according to triple scan method for each material.

Table 3

Mean ± standard deviation RMS (µm) values (95 % confidence interval) of materials that require post-milling firing. AM, Nano-lithium disilicate; EX, Lithium disilicate; TS, Advanced lithium disilicate.

		Overall	External	Intaglio	Marginal
AM	Before post-milling firing	52.7 ± 1.8 <sup>b</sup>	42.3 ± 3.1 <sup>b</sup>	60.9 ± 3.3 <sup>b</sup>	36.7 ± 3.0 <sup>b</sup>
	After post-milling firing	48.1 ± 3.1 <sup>a</sup>	35.2 ± 2.9 <sup>a</sup>	53.5 ± 3.0 <sup>a</sup>	34.2 ± 2.9 <sup>a</sup>
TS	Before post-milling firing	44.5 ± 2.8 <sup>a</sup>	32.6 ± 2.5 <sup>a</sup>	52.3 ± 2.8 <sup>a</sup>	30.5 ± 2.6 <sup>a</sup>
	After post-milling firing	43.3 ± 3.4 <sup>a</sup>	33.2 ± 1.6 <sup>a</sup>	52.0 ± 2.8 <sup>a</sup>	31.3 ± 1.9 <sup>a</sup>
EX	Before post-milling firing	60.2 ± 2.9 <sup>b</sup>	46.1 ± 6.1 <sup>b</sup>	68.7 ± 3.0 <sup>b</sup>	35.1 ± 2.4 <sup>b</sup>
	After post-milling firing	40.6 ± 2.6 <sup>a</sup>	31.9 ± 2.1 <sup>a</sup>	47.9 ± 3.7 <sup>a</sup>	29.7 ± 2.4 <sup>a</sup>

Different superscript lowercase letters indicate significant differences between different conditions of the same material within each surface ( $P < .05$ ).

Table 4

Mean ±standard deviation average gap (µm) values of materials that require post-milling firing. AM, Nano-lithium disilicate; EX, Lithium disilicate; TS, Advanced lithium disilicate.

AM		TS		EX	
Before post-milling firing	After post-milling firing	Before post-milling firing	After post-milling firing	Before post-milling firing	After post-milling firing
149.0 ± 6.0 <sup>b</sup>	115.2 ± 8.3 <sup>a</sup>	102.8 ± 4.8 <sup>a</sup>	102.3 ± 5.4 <sup>a</sup>	147.4 ± 4.8 <sup>b</sup>	108.6 ± 3.8 <sup>a</sup>

Different superscript lowercase letters indicate significant differences between different conditions within each material ( $P < .05$ ).

Table 5

Mean ±standard deviation RMS (µm) values (95 % confidence interval) of each material-surface pair in µm. AM, Nano-lithium disilicate; EX, Lithium disilicate; IN, Fully crystallized lithium disilicate; TS, Advanced lithium disilicate.

	Overall	External	Intaglio	Marginal
AM	48.1 ± 5.1 <sup>b</sup> (44.4–51.8)	35.2 ± 2.9 <sup>b</sup> (33.1–37.2)	53.5 ± 3.0 <sup>b</sup> (51.4–55.6)	34.2 ± 2.9 <sup>b</sup> (32.1–36.3)
IN	43.3 ± 3.1 <sup>a</sup> (41.2–45.5)	32.1 ± 2.4 <sup>a</sup> (30.3–33.8)	51.5 ± 3.6 <sup>ab</sup> (48.9–54.1)	30.4 ± 3.9 <sup>a</sup> (27.8–33.0)
TS	43.3 ± 3.4 <sup>a</sup> (40.8–45.8)	33.2 ± 1.6 <sup>ab</sup> (32.0–34.6)	52.0 ± 2.8 <sup>b</sup> (50.0–54.0)	31.3 ± 1.9 <sup>ab</sup> (29.9–32.7)
EX	40.6 ± 2.6 <sup>a</sup> (38.7–42.5)	31.9 ± 2.1 <sup>a</sup> (30.4–33.4)	47.9 ± 3.7 <sup>a</sup> (45.3–50.5)	29.7 ± 2.4 <sup>a</sup> (28.0–31.4)

Table 6

Mean ± standard deviation and 95 % confidence interval (CI) average gap (µm) values of each material. AM, Nano-lithium disilicate; EX, Lithium disilicate; IN, Fully crystallized lithium disilicate; TS, Advanced lithium disilicate.

	Mean ±standard deviation	95 % CI
AM	115.2 ± 8.3 <sup>b</sup>	109.3–121.1
IN	103.6 ± 6.2 <sup>a</sup>	99.2–108.0
TS	102.8 ± 4.8 <sup>a</sup>	99.3–106.3
EX	108.6 ± 3.8 <sup>ab</sup>	105.9–111.3

Different superscript lowercase letters indicate significant differences among materials ( $P < .05$ ).

(GOM Inspect; GOM, Braunschweig, Germany) was used for deviation analyses. Other studies on the dimensional change of EX after crystallization have used silicone replica technique [12], x-ray microtomography [14], or optical microscopy [15,25] to evaluate the marginal and internal gap; therefore, a direct comparison with the present study might be misleading. Nevertheless, crystallization was reported to both increase [12,14,15,25] and decrease the internal gap [12,14].

The fabrication trueness and internal fit of tested lithium disilicate ceramics had significant differences as AM mostly had higher deviations and higher internal gaps. Therefore, the third and the fourth null hypotheses were rejected. However, it should be emphasized that the greatest mean difference among tested materials when surface deviations were considered was  $7.5\ \mu\text{m}$  (AM and EX), which may be clinically small and negligible. Color maps support this interpretation as all materials had similar color schemes. Clinically undercontoured areas, which are indicated in blue, were evident on the buccal surface of all crowns. In addition, a range of blue color was visible on the interproximal surfaces of AM, IN, and EX, and on the mesial axial surface of TS. However, red was visible on the distal axial wall of TS. Therefore, it can be hypothesized that all crowns would require additional veneering for esthetic purposes, and AM, IN, and EX crowns would require veneering to compensate for possible light or open interproximal contacts, whereas TS crowns would require adjustments on the distal axial wall for tight interproximal contacts. This additional veneering on the buccal surface would also be beneficial for the laterotrusive movements as blue in varying chroma was evident on the buccal inclination of the buccal cusps. The buccal contour of the M-STL might have also contributed to the undercontoured areas as the milling unit might have over-milled this contour to reach the undercut areas. However, this hypothesis needs to be supported with a study on the trueness of lithium disilicate crowns designed on a model with antagonist and adjacent teeth. When the occlusal surfaces were further evaluated, a color scheme with red, yellow, and green was observed for all materials, indicating a possible need for occlusal adjustment. However, considering the small differences among tested materials when overall and external surface deviations were considered, the duration of adjustments may be similar. Color maps of all materials when the intaglio surface was considered were somewhat similar with blue and green colors dominant on the occlusal surface and a range of colors from red to green on the axial surfaces. However, the color map of TS differed from those of other materials with dominant red on the axial walls. Therefore, the clinical duration of intaglio surface adjustments of TS may be longer. Even though the color maps of TS and EX showed overcontoured areas when marginal surface was concerned, the greatest mean difference among materials was  $4.5\ \mu\text{m}$  (AM and EX). This could be interpreted as tested materials having similar marginal gap values; however, this hypothesis needs to be supported with studies on the marginal gap of tested materials evaluated by using different techniques. Given that the greatest mean difference among tested materials when average gap values were considered was  $12.4\ \mu\text{m}$  (AM and TS), which is smaller than the  $80\ \mu\text{m}$  cement gap of M-STL, and the color maps generated after triple scan protocol are parallel to those generated after superimpositions for the intaglio surface, the authors think that the methodology and the results of internal fit analysis are justified. Tested crowns may also have a similar clinical fit after necessary adjustments. However, none of the test groups had a mean average gap value similar to or lower than the  $80\ \mu\text{m}$  cement gap of the M-STL, which could be related to the diameter of the burs used for milling [29]. In different clinical situations that require a higher cement gap value such as an increased number of units or while using advanced cement gap settings of the design software program, tested lithium disilicate ceramics may have higher intaglio surface trueness and lower internal gap values.

A recent study has reported that IN had higher trueness when compared with TS and EX [22]. However, methodological differences elaborated in the second paragraph might have led to these contradictory results. Another study concluded that AM and EX had similar external surface trueness while reporting higher trueness for EX at intaglio and higher trueness for AM at marginal surfaces [23]. The fact that the crowns were digitized by using a laboratory scanner in Kang et al's [23] study may be associated with this difference as the IOS used in the present study allows the digitization of the entire crown with a single movement. However, while using laboratory scanners, separate scans of the external and intaglio surfaces require digital stitching to generate

the STL file of the milled crown. Crystallized EX was shown to have trueness similar to or higher than that of zirconia-reinforced lithium silicate [16], while precrystallized EX was shown to have lower trueness than that of the same zirconia-reinforced lithium silicate [31], which highlights the effect of crystallization on measured deviations. Marginal adaptation of IN, TS, and EX was also investigated by using x-ray microtomography and while EX was reported to have lower marginal gap values regardless of the firing condition, only IN had higher marginal gap values after glaze firing [11].

A limitation of the present study was that the number of tested materials was limited to four and lithium disilicate ceramics from different manufacturers may have different results. Another limitation was that no post-milling processes other than post-milling firing were involved, and additional glazing or polishing may affect measured deviations. It should also be emphasized that all specimens were fired by using the same furnace. These are particularly critical for TS as the mandatory matrix firing may be performed along with glazing and performing these processes by using the proprietary induction furnace of TS' manufacturer may lead to different results considering that the process takes only four and a half minutes [6]. In addition, only one milling unit and one IOS were tested in the present study. IOSs enable the digitization of dental appliances in one rounded motion, which eliminates possible stitching-related inaccuracies that could be encountered if a desktop scanner is used [29]. The tested IOS was reported to have high accuracy [34,35] and precision similar to that of laboratory scanners [36]. Nevertheless, another IOS or a laboratory scanner may affect the results. Another limitation was that only specimens of high translucency were tested in the present study. This may be particularly important for AM as its translucency can be adjusted with firing temperature, and for those situations where a less translucent restoration is required, a higher firing temperature may affect the shrinkage of the restoration. All materials were fabricated by using a standardized milling mode and more detailed modes may lead to different results. Deviation analysis by using compatible software programs [16,22,23,26,27,30–32] and using triple scan protocol to analyze the internal fit has been well-documented [28]. However, the present study did not investigate the marginal adaptation of lithium disilicate ceramics, which can be affected by the cementation process along with material type, and it should be mentioned that analysis methods suitable to evaluate both internal and marginal adaptation have been reported [12,14]. The present study was limited to crowns and different restoration designs may affect the results. Finally, fabrication trueness and internal fit of restorations are not the only clinically relevant parameters that could be affected by the post-milling firing process as mechanical properties may also be affected. Future studies should investigate how further processes such as glazing or polishing affect measured deviations and internal and marginal fit of restorations with different geometries along with how tested parameters change after long-term aging to further elaborate the knowledge on newly introduced lithium disilicate ceramics and their applicability.

## 5. Conclusions

Within the limitations of the present study, the following conclusions were drawn:

1. Post-milling firing of tested lithium disilicate ceramics led to significantly increased fabrication trueness and internal fit, whereas the effect of post-milling firing on the fabrication trueness and internal fit of nano-lithium disilicate ceramic was nonsignificant.
2. Tested nano-lithium disilicate ceramic had fabrication trueness that was similar to or lower than those of other materials. In addition, it mostly had higher internal gaps. However, the mean differences among tested materials were relatively small and may be clinically negligible.

## CRedit authorship contribution statement

**Münir Demirel:** Software, Resources, Methodology, Investigation, Data curation, Conceptualization. **Mustafa Borga Donmez:** Writing – original draft, Validation, Supervision, Conceptualization.

## Declaration of competing interest

The authors declare that they have no known competing financial interests or personal relationships that could have appeared to influence the work reported in this paper.

## Acknowledgment

The authors would like to thank Almira Ada Diken T\374rksayar for their contributions to the formal analysis of the study.

## References

- Y. Chen, A.W.K. Yeung, E.H.N. Pow, J.K.H. Tsoi, Current status and research trends of lithium disilicate in dentistry: a bibliometric analysis, *J. Prosthodont.* 126 (4) (2021) 512–522, <https://doi.org/10.1016/j.prosdent.2020.08.012>.
- C. Abad-Coronel, A. Ordoñez Balladares, J.I. Fajardo, B.J. Martín Biedma, Resistance to fracture of lithium disilicate feldspathic restorations manufactured using a CAD/CAM system and crystallized with different thermal units and programs, *Materials* 14 (12) (2021) 3215, <https://doi.org/10.3390/ma14123215>.
- J. Lubauer, R. Belli, H. Peterlik, K. Hürle, U. Lohbauer, Grasping the lithium hype: insights into modern dental lithium silicate glass-ceramics, *Dent. Mater.* 38 (2) (2022) 318–332, <https://doi.org/10.1016/j.dental.2021.12.013>.
- B. Stawarczyk, A. Mandl, A. Liebermann, Modern CAD/CAM silicate ceramics, their translucency level and impact of hydrothermal aging on translucency, Martens hardness, biaxial flexural strength and their reliability, *J. Mech. Behav. Biomed. Mater.* 118 (2021) 104456, <https://doi.org/10.1016/j.jmbbm.2021.104456>.
- J.H. Phark, S. Duarte Jr, Microstructural considerations for novel lithium disilicate glass ceramics: a review, *J. Esthet. Restor. Dent.* 34 (1) (2022) 92–103, <https://doi.org/10.1111/jerd.12864>.
- M. Demirel, A.A. Diken Türksayar, M.B. Donmez, Translucency, color stability, and biaxial flexural strength of advanced lithium disilicate ceramic after coffee thermocycling, *J. Esthet. Restor. Dent.* 35 (2) (2023) 390–396, <https://doi.org/10.1111/jerd.12960>.
- A.A. Diken Türksayar, M. Demirel, M.B. Donmez, Optical properties, biaxial flexural strength, and reliability of new-generation lithium disilicate glass-ceramics after thermal cycling, *J. Prosthodont.* (2022), <https://doi.org/10.1111/jopr.13632>.
- M.B. Donmez, E.O. Olcay, M. Demirel, Load-to-failure resistance and optical characteristics of nano-lithium disilicate ceramic after different aging processes, *Materials* 15 (11) (2022) 4011, <https://doi.org/10.3390/ma15114011>.
- R. Yin, Y.S. Jang, M.H. Lee, T.S. Bae, Comparative evaluation of mechanical properties and wearability of five CAD/CAM dental blocks, *Materials* 12 (14) (2019) 2252, <https://doi.org/10.3390/ma12142252>.
- M. Rosentritt, A. Schmid, C. Huber, T. Strasser, In vitro mastication simulation and wear test of virgilitite and advanced lithium disilicate ceramics, *Int. J. Prosthodont.* 35 (6) (2022) 770–776, <https://doi.org/10.11607/ijp.7820>.
- K. Kojima, K. Nagaoka, Y. Murata, K. Yamamoto, S. Akiyama, Y. Hokii, F. Fusejima, Marginal adaptation of CAD/CAM milled lithium disilicate glass ceramic crowns, *J. Osseointegr.* 14 (4) (2022) 201–204, <https://doi.org/10.23805/JO.2022.14.04.1>.
- J.H. Kim, S. Oh, S.H. Uhm, Effect of the crystallization process on the marginal and internal gaps of lithium disilicate CAD/CAM crowns, *Biomed. Res. Int.* 2016 (2016) 8635483, <https://doi.org/10.1155/2016/8635483>.
- W. Paquet, L. Tapie, B. Mawussi, P. Boitelle, Volumetric and dimensional accuracy assessment of CAD-CAM-manufactured dental prostheses from different materials, *J. Prosthet. Dent.* 129 (1) (2023) 150–159, <https://doi.org/10.1016/j.prosdent.2021.05.024>.
- B.N. De Freitas, B.S.H. Tonin, A.P. Macedo, T.M.P. Dos Santos, M. De Mattos, T. H. Hotta, W. Matsumoto, Adaptation accuracy of milled lithium disilicate crowns: a 2D and 3D microCT analysis, *J. Esthet. Restor. Dent.* 32 (4) (2020) 403–409, <https://doi.org/10.1111/jerd.12574>.
- S.A. Gold, J.L. Ferracane, J. da Costa, Effect of crystallization firing on marginal gap of CAD/CAM fabricated lithium disilicate crowns, *J. Prosthodont.* 27 (1) (2018) 63–66, <https://doi.org/10.1111/jopr.12638>.
- S.Y. Kang, J.H. Park, J.H. Kim, W.C. Kim, Three-dimensional trueness analysis of ceramic crowns fabricated using a chairside computer-aided design/manufacturing system: an in vitro study, *J. Prosth. Res.* 64 (2) (2020) 152–158, <https://doi.org/10.1016/j.jpor.2019.06.004>.
- C.A. Jurado, T. El-Gendy, J. Hyer, A. Tsujimoto, Color stability of fully- and pre-crystallized chair-side CAD-CAM lithium disilicate restorations after required and additional sintering processes, *J. Adv. Prosthodont.* 14 (1) (2022) 56–62, <https://doi.org/10.4047/jap.2022.14.1.56>.
- A. Liebermann, A. Mandl, M. Eichberger, B. Stawarczyk, Impact of resin composite cement on color of computer-aided design/computer-aided manufacturing ceramics, *J. Esthet. Restor. Dent.* 33 (5) (2021) 786–794, <https://doi.org/10.1111/jerd.12738>.
- M. Alhomoud, J.H. Phark, S. Duarte Jr, Bond strength to different CAD/CAM lithium disilicate reinforced ceramics, *J. Esthet. Restor. Dent.* 35 (1) (2023) 129–137, <https://doi.org/10.1111/jerd.12984>.
- S. Garoushi, E. Säilynoja, P.K. Vallittu, L. Lassila, Fracture-behavior of CAD/CAM ceramic crowns before and after cyclic fatigue aging, *Int. J. Prosthodont.* (2021), <https://doi.org/10.11607/ijp.7207>.
- A. Vichi, Z. Zhao, G. Paolone, N. Scotti, M. Mutahar, C. Goracci, C. Louca, Factory crystallized silicates for monolithic metal-free restorations: a flexural strength and translucency comparison test, *Materials* 15 (21) (2022) 7834, <https://doi.org/10.3390/ma15217834>.
- K. Yamamoto, Y. Murata, K. Nagaoka, S. Akiyama, Y. Hokii, F. Fusejima, Comparison of dimensional accuracy of lithium disilicate CAD/CAM ceramics, *J. Osseointegr.* 14 (4) (2022) 205–208, <https://doi.org/10.23805/JO.2022.14.04.2>.
- S.Y. Kang, J.M. Yu, J.S. Lee, K.S. Park, S.Y. Lee, Evaluation of the milling accuracy of zirconia-reinforced lithium silicate crowns fabricated using the dental medical device system: a three-dimensional analysis, *Materials* 13 (20) (2020) 4680, <https://doi.org/10.3390/ma13204680>.
- F. Ferrini, G. Paolone, G.L. Di Domenico, N. Pagani, E.F. Gherlone, SEM evaluation of the marginal accuracy of zirconia, lithium disilicate, and composite single crowns created by CAD/CAM method: comparative analysis of different materials, *Materials* 16 (6) (2023) 2413, <https://doi.org/10.3390/ma16062413>.
- A. Azarbal, M. Azarbal, R.L. Engelmeier, T.C. Kunkel, Marginal fit comparison of CAD/CAM crowns milled from two different materials, *J. Prosthodont.* 27 (5) (2018) 421–428, <https://doi.org/10.1111/jopr.12683>.
- G. Çakmak, A.M. Rusa, M.B. Donmez, C. Akay, Ç. Kahveci, M. Schimmel, B. Yilmaz, Trueness of crowns fabricated by using additively and subtractively manufactured resin-based CAD-CAM materials, *J. Prosthet. Dent.* (2022), <https://doi.org/10.1016/j.prosdent.2022.10.012>.
- G. Çakmak, A.R. Cuellar, M.B. Donmez, M. Schimmel, S. Abou-Ayash, W.E. Lu, B. Yilmaz, Effect of printing layer thickness on the trueness and margin quality of 3D-printed interim dental crowns, *Appl. Sci.* 11 (19) (2021) 9246, <https://doi.org/10.3390/app11199246>.
- G. Çakmak, D. Agovic, M.B. Donmez, Ç. Kahveci, M.S. de Paula, M. Schimmel, B. Yilmaz, Effect of number of supports and build angle on the fabrication and internal fit accuracy of additively manufactured definitive resin-ceramic hybrid crowns, *J. Dent.* 134 (2023) 104548, <https://doi.org/10.1016/j.jdent.2023.104548>.
- M. Demirel, A.A. Diken Türksayar, M.B. Donmez, Fabrication trueness and internal fit of hybrid abutment crowns fabricated by using additively and subtractively manufactured resins, *J. Dent.* 136 (2023) 104621, <https://doi.org/10.1016/j.jdent.2023.104621>.
- G. Çakmak, M.B. Donmez, A.R. Cuellar, Ç. Kahveci, M. Schimmel, B. Yilmaz, Additive or subtractive manufacturing of crown patterns used for pressing or casting: a trueness analysis, *J. Dent.* 124 (2022) 104221, <https://doi.org/10.1016/j.jdent.2022.104221>.
- K. Son, B.Y. Yu, T.H. Yoon, K.B. Lee, Comparative study of the trueness of the inner surface of crowns fabricated from three types of lithium disilicate blocks, *Appl. Sci.* 9 (9) (2019) 1798, <https://doi.org/10.3390/app9091798>.
- M.B. Donmez, B. Yilmaz, H.I. Yoon, Ç. Kahveci, M. Schimmel, G. Çakmak, Effect of computer-aided design and computer-aided manufacturing technique on the accuracy of fixed partial denture patterns used for casting or pressing, *J. Dent.* 130 (2023) 104434, <https://doi.org/10.1016/j.jdent.2023.104434>.
- W.S. Lin, B.T. Harris, D. Morton, Trial insertion procedure for milled lithium disilicate restorations in the precrystallized state, *J. Prosthodont.* 107 (1) (2012) 59–62, [https://doi.org/10.1016/S0022-3913\(12\)60020-1](https://doi.org/10.1016/S0022-3913(12)60020-1).
- M.B. Donmez, V.R. Marques, G. Çakmak, H. Yilmaz, M. Schimmel, B. Yilmaz, Congruence between the meshes of a combined healing abutment-scan body system acquired with four different intraoral scanners and the corresponding library file: an in vitro analysis, *J. Dent.* 118 (2022) 103938, <https://doi.org/10.1016/j.jdent.2021.103938>.
- I. Róth, A. Czigola, D. Fehér, V. Vitai, G.L. Joós-Kovács, P. Hermann, J. Borbély, B. Vecsei, Digital intraoral scanner devices: a validation study based on common evaluation criteria, *BMC Oral Health* 22 (1) (2022) 140, <https://doi.org/10.1186/s12903-022-02176-4>.
- A.B. Nulty, A comparison of full arch trueness and precision of nine intra-oral digital scanners and four lab digital scanners, *Dent. J.* 9 (2021) 75, <https://doi.org/10.3390/dj9070075>.